J. Fluid Mech. (2020), *vol*. 899, A25. © The Author(s), 2020.
Published by Cambridge University Press
doi:10.1017/jfm.2020.459

Fokker–Planck model for binary mixtures

Samarth Agrawal[1], **S. K. Singh**[1] **and S. Ansumali**[1,†]

[1]Engineering Mechanics Unit, Jawaharlal Nehru Centre for Advanced Scientific Research, Jakkur, Bangalore 560064, India

(Received 19 October 2019; revised 4 March 2020; accepted 26 May 2020)

The Fokker–Planck approximation to the Boltzmann equation has emerged as an efficient alternative to the discrete simulation Monte Carlo method for various flow simulations. This method has been mostly limited to simulating single-component rarefied gas flows. In the present paper, we propose two models based on the Fokker–Planck equation and quasi-equilibrium models that are capable of describing the dynamics of rarefied binary gas mixtures over a large range of Schmidt numbers. We first prove that these models satisfy the necessary conservation laws and the H-theorem. We validate the model by simulating three benchmark problems – Graham's law for effusion, Couette flow and binary diffusion.

Key words: kinetic theory

1. Introduction

Fluid dynamics for gases at continuum scale, i.e. when system size is much larger than the mean free path, is well described by the Navier–Stokes–Fourier dynamics. In this description, one assumes that the system is locally close to thermodynamic equilibrium. A more general description of dilute gas dynamics is provided by the Boltzmann equation, which describes the dynamics even far away from thermodynamic equilibrium and at all Knudsen numbers, defined as $Kn = \lambda/L$, where λ is the mean free path and L is the characteristic length of the system (Grad 1949; Chapman & Cowling 1970). In the kinetic theory of gases, as developed by Boltzmann and Maxwell, one assumes gases to be composed of structureless point particles and provides a statistical description of the motion of the particles in terms of the single-particle distribution function. The Boltzmann equation is the time evolution equation for the distribution function, where time evolution is represented as a sequence of free flights and binary collisions described by an integro-differential term. Given the complex nonlinear integro-differential form of the collision term, there is a long history in kinetic theory of representing the collision term via model dynamics. Perhaps the most famous and widely used one is the Bhatnagar–Gross–Krook (BGK) model (Bhatnagar, Gross & Krook 1954), where one assumes that complex collision terms can be replaced by a relaxation dynamics towards an equilibrium Maxwell–Boltzmann distribution. The BGK model has correct hydrodynamic limit of Navier–Stokes–Fourier dynamics and thermodynamic consistency with the Boltzmann equation as described by the H-theorem. However, as the model

† Email address for correspondence: ansumali@jncasr.ac.in

https://doi.org/10.1017/jfm.2020.459 Published online by Cambridge University Press

describes relaxation towards a Maxwell–Boltzmann distribution by a single relaxation time, all non-conserved moments, such as the stress and heat flux, relax at the same rate. Thus, the BGK model is incapable of accurately modelling all the transport coefficients and thus predicts the Prandtl number (ratio of thermal and momentum diffusion times) of dilute gases as unity in place of $2/3$. More sophisticated models, such as the ellipsoidal statistical Bhatnagar–Gross–Krook (ES-BGK) model, do not have such defects (Holway 1966). Constructing model collision dynamics of relaxation type, which preserves both hydrodynamic and thermodynamic consistency, is well understood for both a single-component gas and multi-component gas mixtures (Gorban & Karlin 1994*a*).

Lebowitz, Frisch & Helfand (1960) proposed an alternative framework for the collision model by proposing that the relaxation of an arbitrary distribution towards the Maxwell–Boltzmann distribution can also be modelled as a Fokker–Planck like diffusive process in velocity space. Even though this model has the correct hydrodynamic limit (with Prandtl number $3/2$) and satisfies the H-theorem, it has rarely been used for rarefied gas dynamics applications until recently. This model has seen a revived interest in the last decade owing to the fact that the Fokker–Planck model has an equivalent Langevin dynamics which can be efficiently discretized (Gorji & Jenny 2014). Recently, it was shown that the Prandtl-number defect can be cured without compromising on its thermodynamic consistency by two independent methodologies. Gorji & Jenny (2012) introduced a generalized nonlinear Fokker–Planck model to correct the Prandtl number, while Singh & Ansumali (2015) showed that the Prandtl number can be tuned by changing the drift term in the Fokker–Planck model. These recent advances have successfully enabled the kinetic modelling of gases for boundary value problems pertaining to engineering via the Fokker–Planck approximation (Gorji, Torrilhon & Jenny 2011; Singh, Thantanapally & Ansumali 2016). However, this is limited to the single-component case, and techniques dealing with gas mixtures have not attained the same level of sophistication. Recently, Gorji & Jenny (2012) introduced a generalized nonlinear Fokker–Planck model for gas mixtures that correctly describes the conservation of mass, momentum and energy, and the transfer between the components as well, and they also managed to recover the relevant transport coefficients. However, as of now, there is no proof available for the thermodynamic consistency of this model. In the present paper, we present an alternative approach based on quasi-equilibrium models to introduce a Fokker–Planck model for binary mixtures and verify the veracity of this model through some basic simulations.

The paper is organized as follows. The distribution function and macroscopic variables are introduced in § 2. In § 3, we explain the Boltzmann equation and its basic properties for rarefied gases. Following this, various approximations to the Boltzmann collisional kernel, including the BGK approximation, quasi-equilibrium models and the Fokker–Planck approximation for hydrodynamics, are explained. In §§ 4 and 5, the Boltzmann equation for binary mixtures and quasi-equilibrium distribution functions for the same are described. Based on these ideas, we introduce two Fokker–Planck models for different Schmidt numbers. Transport coefficients for these models are calculated in § 6. Following this, we outline the numerical solution algorithm of the resulting Fokker–Planck equations in § 7. Finally, in § 8 we discuss the various benchmark problems that were used to validate these models.

2. The distribution function and macroscopic variables

The kinetic theory of gases provides a statistical description of the motion of molecules in terms of the distribution function, $f(\boldsymbol{x}, \boldsymbol{c}, t)$, which is the probability density of finding

https://doi.org/10.1017/jfm.2020.459 Published online by Cambridge University Press

a particle in an infinitesimal volume element d$\boldsymbol{x}$ containing the point $\boldsymbol{x}$ with a velocity in the range of d$\boldsymbol{c}$ about the point $\boldsymbol{c}$, where $\boldsymbol{x}$ and $\boldsymbol{c}$ are position and molecular velocity, respectively (Chapman & Cowling 1970). Similarly, for an $\mathcal{N}$-component mixture the description is provided in terms of $f_i(\boldsymbol{x}, \boldsymbol{c}, t)\,\mathrm{d}\boldsymbol{x}\,\mathrm{d}\boldsymbol{c}$, which is the probability of finding a particle of the ith type in the neighbourhood of $(\boldsymbol{x}, \boldsymbol{c})$. The relevant macroscopic quantities can then be found by taking the appropriate moment of the distribution function. The component number density n_i and the mixture number density n are

$$n_i = \langle 1, f_i \rangle, \quad n = \sum_i n_i, \tag{2.1a,b}$$

where the summation is over all components and the $\langle \phi_1, \phi_2 \rangle$ operator is

$$\langle \phi_1(\boldsymbol{c}_i), \phi_2(\boldsymbol{c}_i) \rangle = \int_{-\infty}^{\infty} \phi_1(\boldsymbol{c}_i)\phi_2(\boldsymbol{c}_i)\,\mathrm{d}\boldsymbol{c}_i. \tag{2.2}$$

A convention of explicit summation over all components is used for mixture quantities. As an example, the mixture density is defined as $\rho = \sum_i \rho_i$, where the component mass density is defined as $\rho_i = m_i n_i$ with m_i being the mass of each particle of the ith component. Similarly, in D dimensions, the momentum $\rho\boldsymbol{u}$, the energy E and the temperature T of the mixture are defined as

$$\rho\boldsymbol{u} = \sum_i \langle m_i \boldsymbol{c}_i, f_i \rangle, \quad E = \sum_i \left\langle \frac{m_i c_i^2}{2}, f_i \right\rangle, \quad \frac{D}{2} n k_B T = \sum_i \left\langle \frac{m_i (\boldsymbol{c}_i - \boldsymbol{u})^2}{2}, f_i \right\rangle, \tag{2.3a–c}$$

where k_B is the Boltzmann constant. Similar to the single-component case, the component velocity $\boldsymbol{u}_i$ and component temperature T_i are

$$\rho_i \boldsymbol{u}_i = \langle m_i \boldsymbol{c}_i, f_i \rangle, \quad \frac{D}{2} n_i k_B T_i = \left\langle \frac{m_i (\boldsymbol{c}_i - \boldsymbol{u}_i)^2}{2}, f_i \right\rangle. \tag{2.4a,b}$$

Similarly the pressure p, the stress $\sigma_{\alpha\beta}$ and the heat flux q_α are

$$p = \sum_i n_i k_B T, \quad \sigma_{\alpha\beta} = \sum_i \left\langle m_i \overline{\xi_{i\alpha}\xi_{i\beta}}, f_i \right\rangle, \quad q_\alpha = \sum_i \left\langle m_i \frac{\xi_i^2}{2} \xi_{i\alpha}, f_i \right\rangle, \tag{2.5a–c}$$

where $\xi_{i\alpha} = c_{i\alpha} - u_\alpha$ and with $\overline{A_{\alpha\beta}}$ indicating the traceless part of the tensor.

At equilibrium, the distribution function attains the Maxwell–Boltzmann distribution form

$$f_i^{MB} = n_i \left(\frac{m_i}{2\pi k_B T} \right)^{D/2} \exp\left(-\frac{m_i}{2k_B T} (\boldsymbol{c}_i - \boldsymbol{u})^2 \right). \tag{2.6}$$

The component velocities and temperatures assume the values of their mixture counterparts, while the stress and heat flux become zero at equilibrium, that is

$$\boldsymbol{u}_i[f^{MB}] = \boldsymbol{u}, \quad T_i[f^{MB}] = T, \quad \sigma_{\alpha\beta}[f^{MB}] = 0, \quad q_\alpha[f^{MB}] = 0. \tag{2.7a–d}$$

The kinetic theory of gases also extends the idea of entropy present in statistical mechanics to non-equilibrium situations. This is achieved via the H-function defined as

$$H = \sum_i \int \mathrm{d}\boldsymbol{c}_i\, (f_i \ln f_i - f_i). \tag{2.8}$$

https://doi.org/10.1017/jfm.2020.459 Published online by Cambridge University Press

It can be shown that the H-function steadily decreases as the system progresses in time and at equilibrium attains a form similar to the Sackur–Tetrode expression of entropy in thermodynamics (Chapman & Cowling 1970), as $S_B = -k_B H[f^{MB}]$, wherein

$$H[f^{MB}] = \sum_i n_i \left[\frac{D}{2} \log \frac{2\pi k_B T}{m_i} - \log n_i + \frac{D}{2} \right], \tag{2.9}$$

which shows that kinetic theory is consistent with features of statistical mechanics. This completes the description of the various relevant macroscopic quantities that are calculated from the distribution function and their behaviour at equilibrium.

3. The Boltzmann equation

For the case of dilute gases, the time evolution of the distribution function is described by the Boltzmann equation (Chapman & Cowling 1970). For the single-component dilute gas, the Boltzmann equation has the form

$$\partial_t f(\boldsymbol{x}, \boldsymbol{c}, t) + c_\alpha \partial_{x_\alpha} f(\boldsymbol{x}, \boldsymbol{c}, t) = \Omega, \tag{3.1}$$

where Ω is a term that accounts for the change due to collisions between particles. The Boltzmann collisional operator, Ω^B, quantifies the change in the distribution function from all possible binary collisions, and is expressed as

$$\Omega^B = \iiint [w' f(\boldsymbol{x}, \boldsymbol{c}', t) f(\boldsymbol{x}, \boldsymbol{c}_1', t) - w f(\boldsymbol{x}, \boldsymbol{c}, t) f(\boldsymbol{x}, \boldsymbol{c}_1, t)] \, \mathrm{d}\boldsymbol{c}_1 \, \mathrm{d}\boldsymbol{c}' \, \mathrm{d}\boldsymbol{c}_1', \tag{3.2}$$

where $w \equiv w(\boldsymbol{c}', \boldsymbol{c}_1'; \boldsymbol{c}, \boldsymbol{c}_1)$ is the probability of the colliding pair to transition from the velocities $(\boldsymbol{c}, \boldsymbol{c}_1)$ to $(\boldsymbol{c}', \boldsymbol{c}_1')$ and *vice versa* for w', and it can be shown that $w = w'$ (Lifschitz & Pitaevskii 1981). The first term of the integrand represents the increase (gain) in the value of the distribution function $f(\boldsymbol{x}, \boldsymbol{c}, t)$ and similarly the second term represents the decrease (loss). In order to satisfy the conservation of momentum and energy, the velocity pairs must satisfy

$$\boldsymbol{c} + \boldsymbol{c}_1 = \boldsymbol{c}' + \boldsymbol{c}_1', \quad c^2 + c_1^2 = c'^2 + c_1'^2. \tag{3.3a,b}$$

Therefore, by integrating over all possible $(\boldsymbol{c}_1, \boldsymbol{c}', \boldsymbol{c}_1')$, the total change in $f(\boldsymbol{x}, \boldsymbol{c}, t)$ from collisions can be calculated. Further, by considering appropriate moments and integrating over the velocity space, the dynamics of various macroscopic quantities can be derived (Grad 1949; Chapman & Cowling 1970).

The Boltzmann equation is a highly complex integro-differential equation and hence does not lend itself to analysis even for simple boundary value problems. Therefore, approximations are made to the collisional term in order to find solutions to the equation. A simple, yet highly useful, model is the BGK approximation (Bhatnagar *et al.* 1954), where the Boltzmann collisional operator is modelled as an approach to the equilibrium distribution function. The BGK collisional operator is

$$\Omega^{BGK} = \frac{1}{\tau_{BGK}} (f^{MB} - f), \tag{3.4}$$

where τ_{BGK} is the relaxation time.

https://doi.org/10.1017/jfm.2020.459 Published online by Cambridge University Press

A variant of this approach is the ES-BGK model (Holway 1966), which has the form

$$\Omega^{ES} = \frac{1}{\tau_{ES}}(f^{ES} - f), \tag{3.5}$$

where τ_{ES} is the relaxation time associated with this model and f^{ES} is the anisotropic Gaussian with the form

$$f^{ES} = \frac{n}{\sqrt{\det[2\pi\lambda_{\alpha\beta}]}} \exp\left(-\frac{1}{2}\xi_\alpha \lambda^{-1}_{\alpha\beta}\xi_\beta\right), \tag{3.6}$$

where det[ ] is the determinant and $\lambda_{\alpha\beta}$ is

$$\lambda_{\alpha\beta} = \frac{k_B T}{m}\delta_{\alpha\beta} + b\frac{\sigma_{\alpha\beta}}{\rho}, \tag{3.7}$$

where the b parameter is used to tune the Prandtl number, as opposed to the BGK model where the Prandtl number is set to 1.

Another method of approximation is the Fokker–Planck operator (Lebowitz *et al.* 1960), wherein the approach to equilibrium is modelled as drift and diffusion dynamics

$$\Omega^{FP} = \frac{1}{\tau_{FP}}\partial_{c_\alpha}\left(\xi_\alpha f + \frac{k_B T}{m}\frac{\partial f}{\partial c_\alpha}\right) = \frac{1}{\tau_{FP}}\frac{k_B T}{m}\partial_{c_\alpha}(f\partial_{c_\alpha}(\ln f - \ln f^{MB})), \tag{3.8}$$

which is essentially the diffusion dynamics in velocity space, with ξ_α acting as the drift coefficient, $k_B T/m$ assumes the role of diffusion coefficient and τ_{FP}^{-1} is the friction constant. It has been shown recently that this approximation is a useful alternative to methods such as discrete simulation Monte Carlo (DSMC) for simulating moderately high-Kn flows.

The Boltzmann equation and its aforementioned approximations are shown to have the following properties

(*a*) *Conservation laws*: As binary collisions do not change the mass, momentum or energy of the system, we have

$$\langle \Omega, \{m, m\boldsymbol{c}, mc^2/2\}\rangle = \{0, \boldsymbol{0}, 0\}. \tag{3.9}$$

Using this result and calculating appropriate moments of the Boltzmann equation, the conservation laws are

$$\left.\begin{aligned} \partial_t \rho + \partial_\alpha \rho u_\alpha &= 0, \\ \partial_t \rho u_\alpha + \partial_\beta(\rho u_\alpha u_\beta + p\delta_{\alpha\beta}) + \partial_\beta \sigma_{\alpha\beta} &= 0, \\ \partial_t E + \partial_\alpha((E+p)u_\alpha + \sigma_{\alpha\gamma}u_\gamma) + \partial_\alpha q_\alpha &= 0, \end{aligned}\right\} \tag{3.10}$$

which are in accordance with the macroscopic laws of conservation.

(*b*) *Zero of the collision*: When the collisions between particles do not affect the state of the system, it reaches a state of equilibrium:

$$\Omega = 0 \quad \Longrightarrow \quad f = f^{MB}. \tag{3.11}$$

The converse is also true, i.e. when $f = f^{MB}$ then $\Omega = 0$.

https://doi.org/10.1017/jfm.2020.459 Published online by Cambridge University Press

(*c*) *H-theorem*: The Boltzmann equation extends the idea of entropy to non-equilibrium situations. This is highlighted from the evolution of the H-function,

$$\partial_t H + \partial_\alpha J_\alpha = -\sigma^S, \tag{3.12}$$

where the H-function is $\langle(\ln f - 1), f\rangle$, J_α is the entropy flux term and $\sigma^S = \langle \Omega, \ln f\rangle$ is the entropy generation term. The Boltzmann collisional operator, the BGK and Fokker–Planck approximations ensure that

$$\sigma^S \geq 0. \tag{3.13}$$

Entropy production is greater than or equal to zero and hence the Boltzmann equation for rarefied gases is in accordance with the laws of thermodynamics. It is also noted that entropy production is zero at equilibrium, that is, when $f = f^{MB}$.

This concisely summarizes the features of the Boltzmann equation and its approximations for the single-component case. In the following section, we briefly explain the Boltzmann equation for binary mixtures, and some well-known approximations, and outline their important features.

4. Kinetic modelling of binary mixtures

The dynamics of binary mixtures is fundamentally different from the single-component case, as the two components exchange momentum and energy through collisions. Hence the Boltzmann equation for binary mixtures considers the different collisional possibilities, as schematically shown in figure 1. The changes in distribution of component A arise from A–A and A–B type collisions, and *vice versa* for component B. As a result, the mixture momentum and energy are conserved as opposed to their componentwise counterparts, i.e.

$$m_A \boldsymbol{c}_A + m_B \boldsymbol{c}_B = m_A \boldsymbol{c}'_A + m_B \boldsymbol{c}'_B, \quad m_A c_A^2 + m_B c_B^2 = m_A c_A'^2 + m_B c_B'^2, \tag{4.1a,b}$$

where m_A and m_B are the mass of A-type and B-type particles, respectively. Here $\boldsymbol{c}$ and $\boldsymbol{c}'$ with a subscript denote the pre-collision and post-collision velocities of the respective particles. The Boltzmann equation for binary mixtures is (Chapman & Cowling 1970)

$$\left.\begin{aligned} \frac{\partial f_A}{\partial t} + c_{A\alpha}\frac{\partial f_A}{\partial x_\alpha} &= \Omega_A^B = \underbrace{\Omega^B(f_A, f_A)}_{\textit{self-collision}} + \underbrace{\Omega^B(f_A, f_B)}_{\textit{cross-collision}}, \\ \frac{\partial f_B}{\partial t} + c_{B\alpha}\frac{\partial f_B}{\partial x_\alpha} &= \Omega_B^B = \underbrace{\Omega^B(f_B, f_B)}_{\textit{self-collision}} + \underbrace{\Omega^B(f_B, f_A)}_{\textit{cross-collision}}, \end{aligned}\right\} \tag{4.2}$$

where the right-hand side of each equation is the change in distribution of the respective component arising from self-collisions represented by $\Omega^B(f_i, f_i)$ and cross-collisions represented by $\Omega^B(f_i, f_j)$. Similar to the single-component case, the evolution equation of various macroscopic variables can be derived using this equation. The collisional operator has the following properties, which should ideally be satisfied by its approximations.

https://doi.org/10.1017/jfm.2020.459 Published online by Cambridge University Press

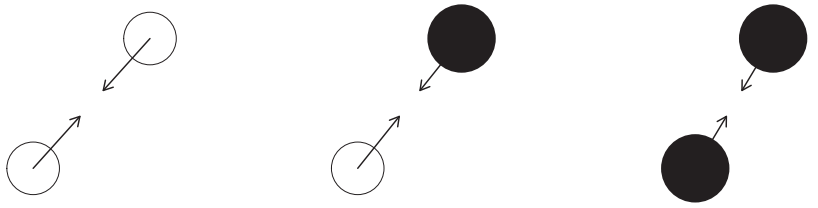


FIGURE 1. The three types of collisional possibilities: A–A, A–B and B–B.

(*a*) *Conservation laws*: The mass of individual species as well as the total momentum and energy of the mixture are conserved, as binary collisions do not contribute any change to these quantities. This is represented as

$$\left\langle \Omega_i^B, \left\{ m_i, \sum_{i=A,B} m_i \boldsymbol{c}_i, \sum_{i=A,B} m_i \frac{c_i^2}{2} \right\} \right\rangle = \{0, \boldsymbol{0}, 0\}, \tag{4.3}$$

using which the conservation laws can be calculated similarly to the single-component case. However, the componentwise momentum and energy are not conserved, as the two components exchange momentum and energy between themselves through cross-collisions (A–B type collisions). It is, in fact, these collisions that facilitate the relaxation of the component momentum and energy to the mixture momentum and energy (Hamel 1965). The mixture variables adhere to the conservation laws as mentioned in (3.10).

(*b*) *Equilibrium*: Similar to the single-component case, the system reaches a state of statistical equilibrium. The distribution of any component i at equilibrium is

$$f_i^{MB} = n_i \left(\frac{m_i}{2\pi k_B T} \right)^{3/2} \exp\left(-\frac{m_i}{2k_B T} (\boldsymbol{c}_i - \boldsymbol{u})^2 \right). \tag{4.4}$$

The converse is also true, i.e. when $\Omega_i^B = 0$ then the distribution function attains the form $f = f_i^{MB}$.

(*c*) *H-theorem*: The Boltzmann collision kernel for binary mixtures satisfies the H-theorem, that is, $\sigma^{(s)} \geq 0$ similar to the single-component case.

(*d*) *Indifferentiability principle*: The equations should adhere to the indifferentiability principle, i.e. the equation should converge to the single-component case for $m_A = m_B$.

Similar to the single-component case, the corresponding BGK collision kernel for a binary mixture is

$$\Omega^{BGK} = \frac{1}{\tau}(f_i^{MB}(\rho_i, \boldsymbol{u}, T) - f_i). \tag{4.5}$$

The fundamental drawback with such a model is that there is only a single relaxation rate for all quantities, whereas, for the case of a binary mixture, there are two important time scales present in the system – the rate of mass diffusion and the rate of momentum diffusion. The dimensionless parameter that is used to characterize these time scales is

https://doi.org/10.1017/jfm.2020.459 Published online by Cambridge University Press

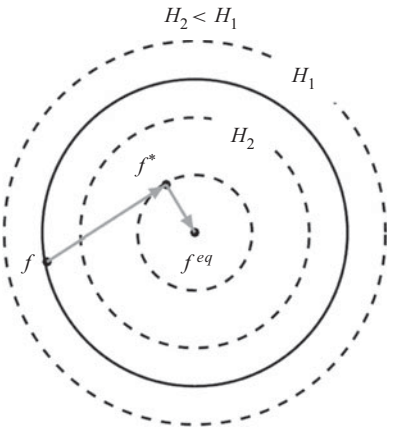


FIGURE 2. Trajectory of the distribution function in a quasi-equilibrium model. The various concentric circles depict different levels of H.

known as the Schmidt number and is defined as (Bergman *et al.* 2011)

$$Sc = \frac{\text{viscous diffusion rate}}{\text{mass diffusion rate}} = \frac{\mu}{\rho D_{AB}}, \tag{4.6}$$

where μ is the viscosity, ρ is the density and D_{AB} is the mass diffusion coefficient. For such an approximation, $Sc = 1$ for all cases, and hence does not manage to accurately describe the system. Therefore, the collision kernel should be approximated in a manner capable of preserving these different time scales.

Various approaches to correct this defect exist. In order to deal with multiple time scales, the basic idea of fast–slow decomposition of motions near the quasi-equilibrium was introduced (Gorban & Karlin 1994*a*,*b*; Levermore 1996). In accordance with this idea, the relaxation to equilibrium is modelled as a two-step process, where 'fast' relaxation happens from the initial to the quasi-equilibrium state and 'slow' relaxation happens from the quasi-equilibrium state to the final equilibrium state. In the context of multiple time scales, the quasi-equilibrium models are a simple alternative (Gorban & Karlin 1994*a*,*b*; Levermore 1996) to the BGK approximation which can effectively incorporate multiple time scales of the system. The collision kernel for the quasi-equilibrium model is

$$\Omega_i^{QE} = \frac{1}{\tau_1}(f_i^*(M^{quasi\text{-}slow}, M^{slow}) - f_i) + \frac{1}{\tau_2}(f_i^{MB}(M^{slow}) - f_i^*(M^{quasi\text{-}slow}, M^{slow})), \tag{4.7}$$

where $f_i^*(M^{quasi\text{-}slow}, M^{slow})$ is the quasi-equilibrium distribution function and is a function of the quasi-slow moments $M^{quasi\text{-}slow}$ and the slow moments M^{slow} (Gorban & Karlin 1994*b*; Levermore 1996). The idea is that the system moves towards a state of quasi-equilibrium, where the quasi-slow moments relax first, and then proceeds towards equilibrium, where the slow moments react; a visual description of the idea is presented in figure 2. Similar to the approach adopted by Arcidiacono *et al.* (2007), two possible forms for the quasi-equilibrium distribution are constructed: for low Sc where mass diffusion occurs at a higher rate as compared to momentum diffusion, and *vice versa* for high Sc.

The two distinct regimes of the Schmidt number can be explained at a kinetic level in the following manner.

https://doi.org/10.1017/jfm.2020.459 Published online by Cambridge University Press

(*a*) When the self-collisions (A–A and B–B types) dominate and have shorter time scales, the low-Schmidt-number regime is observed. In this case, the individual species first relax to the Maxwell–Boltzmann distribution corresponding to the component velocity and temperature, following which they relax to the Maxwell–Boltzmann distribution with mixture velocity and temperature at longer time scales.

(*b*) When the cross-collisions (A–B type) have a shorter characteristic time scale, the system has a higher Schmidt number, as the particles of different species collide at a higher rate and exchange momentum and energy, thereby initially relaxing to the mixture velocity and temperature and over a long time attain the Maxwell–Boltzmann distribution.

For the first case, the physically relevant quasi-slow variables are

$$M^{quasi\text{-}slow} = \{\rho_i,\, \rho_i \boldsymbol{u}_i,\, n_i k_B T_i\}, \tag{4.8}$$

which imposes the following condition on the quasi-equilibrium distribution function f_i^*:

$$\left\langle \left\{ m_i,\, m_i \boldsymbol{c}_i,\, m_i \frac{(\boldsymbol{c}_i - \boldsymbol{u}_i)^2}{2} \right\}, f_i^* \right\rangle = \left\{ \rho_i,\, \rho_i \boldsymbol{u}_i,\, \frac{3}{2} n_i k_B T_i \right\}. \tag{4.9}$$

By minimizing the H-function as defined in (2.8) under these constraints, the form of quasi-equilibrium for the low-Schmidt-number limit, $f_i^{*(L)}$,is (Arcidiacono *et al.* 2006)

$$f_i^{*(L)} = n_i \left(\frac{m_i}{2\pi k_B T_i} \right)^{3/2} \exp\left(-\frac{m_i (c_i - u_i)^2}{2 k_B T_i} \right). \tag{4.10}$$

Similarly, for the second case where the momentum diffuses faster, the set of constraints under which the H-function is to be minimized is

$$\left\langle \left\{ m_i,\, m_i \boldsymbol{c}_i,\, \sum_{i=A,B} m_i \xi_{i\alpha} \xi_{i\beta} \right\}, f_i^* \right\rangle = \{\rho_i,\, \rho_i \boldsymbol{u},\, n\theta_{\alpha\beta}\}, \tag{4.11}$$

where

$$\theta_{\alpha\beta} = \frac{1}{n} \sum_{i=A,B} \left\langle m_i \xi_{i\alpha} \xi_{i\beta}, f_i \right\rangle. \tag{4.12}$$

The quasi-equilibrium distribution function for the high-Schmidt-number limit, $f_i^{*(H)}$, is (Arcidiacono *et al.* 2006)

$$f_i^{*(H)} = n_i \left(\frac{m_i}{2\pi |\theta_{\alpha\beta}|} \right)^{3/2} \exp\left(\frac{-m_i \xi_{i\alpha} \theta_{\alpha\beta}^{-1} \xi_{i\beta}}{2} \right), \tag{4.13}$$

where $|\theta_{\alpha\beta}|$ is the determinant.

These two distinct forms of quasi-equilibrium can be used to build two different collision kernels based on the Fokker–Planck approximation, which can be solved for binary mixtures.

https://doi.org/10.1017/jfm.2020.459 Published online by Cambridge University Press

5. Quasi-equilibrium models for Fokker–Planck formulation

The Fokker–Planck approximation to the Boltzmann equation of the form (3.8) involves only a single time scale and therefore is not well suited for modelling systems with multiple time scales. To resolve this problem, Gorji & Jenny (2012) proposed a model that could account for the different collision frequencies and with a cubic drift term that enabled correct calculation of the transport coefficients. We propose to extend the Fokker–Planck approximation for binary mixtures by incorporating the concept of quasi-equilibrium models in a manner that would correctly represent the multiple time scales present in the system and its approach to equilibrium.

From (3.8), the Fokker–Planck approximation is

$$\Omega^{FP} = \frac{1}{\tau_{FP}} \frac{k_B T}{m} \partial_{c_\alpha} (f \partial_{c_\alpha} (\ln f - \ln f^{MB})). \tag{5.1}$$

This form of the Fokker–Planck model better illustrates the approach of the Maxwell–Boltzmann distribution, similar to the BGK model. In order to build a quasi-equilibrium like model with multiple time scales, we extend the Fokker–Planck model for it to have a similar form. Here, the approach to equilibrium is defined as a two-step process wherein the first term represents a logarithmic approach to quasi-equilibrium and the second to equilibrium:

$$\Omega_i^{FP} = \left(\frac{1}{\tau_1} - \frac{1}{\tau_2} \right) A_{\alpha\beta} \partial_{c_{i\beta}} (f_i \partial_{c_{i\alpha}} (\ln f_i - \ln f_i^*)) + \frac{1}{\tau_2} \frac{k_B T}{m_i} \partial_{c_{i\alpha}} (f_i \partial_{c_{i\alpha}} (\ln f_i - \ln f_i^{MB})), \tag{5.2}$$

where τ_1 and τ_2 are the characteristic time scales associated with the approach to quasi-equilibrium and equilibrium, and $A_{\alpha\beta}$ is the diffusion coefficient that relaxes the system to the quasi-equilibrium state, for the low-Schmidt-number dynamics; $A_{\alpha\beta}$ can be chosen as $A_{\alpha\beta} = (k_B T_i / m_i) \delta_{\alpha\beta}$. Using the form of f_i^* presented in (4.10), the collision kernel for the low-Schmidt-number limit is

$$\Omega_i^{FP(L)} = \frac{1}{\tau_1} \partial_{c_{i\alpha}} \left((c_{i\alpha} - u_{i\alpha}) f_i + \frac{k_B T_i}{m_i} \frac{\partial f_i}{\partial c_{i\alpha}} \right) + \frac{1}{\tau_2} \partial_{c_{i\alpha}} \left((u_{i\alpha} - u_\alpha) f_i + \frac{k_B \Delta T}{m_i} \frac{\partial f_i}{\partial c_{i\alpha}} \right), \tag{5.3}$$

where $\Delta T = T - T_i$ is the difference in component and mixture temperatures.

Similarly, for the high-Schmidt-number dynamics, $A_{\alpha\beta}$ is taken as $A_{\alpha\beta} = \theta_{\alpha\beta}$, and the collision kernel for the high-Schmidt-number limit is

$$\Omega_i^{FP(H)} = \frac{1}{\tau_1} \partial_{c_{i\alpha}} \left((c_{i\alpha} - u_\alpha) f_i + \frac{\theta_{\alpha\beta}}{m_i} \frac{\partial f_i}{\partial c_{i\beta}} \right) + \frac{1}{\tau_2} \partial_{c_{i\alpha}} \left(\left(\frac{k_B T \delta_{\alpha\beta}}{m_i} - \frac{\theta_{\alpha\beta}}{m_i} \right) \frac{\partial f_i}{\partial c_{i\beta}} \right). \tag{5.4}$$

For this model to be considered canonical, it must satisfy the properties of collision as mentioned in § 4. By integrating over the velocity space $\boldsymbol{c}_i$, it can be verified that the quasi-equilibrium Fokker–Planck model satisfies the constraints of (4.3). The evolution equations for component mass, mixture momentum and energy are the same as the conservation laws mentioned in (3.10). Furthermore, the component momentum and

https://doi.org/10.1017/jfm.2020.459 Published online by Cambridge University Press

energy equations in relaxation form are

$$\left.\begin{aligned}\left\langle \Omega_i^{FP(L)}, m_i c_{i\alpha} \right\rangle &= \frac{1}{\tau_2}(\rho_i u_\alpha - \rho_i u_{i\alpha}),\\ \left\langle \Omega_i^{FP(L)}, \frac{m_i c_i^2}{2} \right\rangle &= \frac{1}{\tau_2}(\rho_i u_{i\alpha}(u_\alpha - u_{i\alpha}) + Dk_B n_i(T - T_i)),\end{aligned}\right\} \tag{5.5}$$

for the low-Schmidt-number case. Similarly, for the high-Schmidt-number case the relaxation equations for component momentum and energy are

$$\left.\begin{aligned}\left\langle \Omega_i^{FP(H)}, m_i c_{i\alpha} \right\rangle &= \frac{1}{\tau_1}(\rho_i u_\alpha - \rho_i u_{i\alpha}),\\ \left\langle \Omega_i^{FP(H)}, \frac{m_i c_i^2}{2} \right\rangle &= \frac{1}{\tau_1}(\rho_i u_{i\alpha}(u_\alpha - u_{i\alpha}) + Dk_B n_i(T - T_i)).\end{aligned}\right\} \tag{5.6}$$

If $\tau_1 \leq \tau_2$, the component velocities equilibrate faster in the second case than in the first, which is as expected since the second model is applicable for the high-Schmidt-number regime wherein the viscous diffusion rate dominates the mass diffusion rate.

For the proposed model, the expression for entropy generation (σ^S) is

$$\sigma^S = \frac{1}{\tau_{eff}} \sum_i -Dn_i + \int \frac{1}{f_i}\frac{\partial f_i}{\partial c_{i\alpha}} A_{\alpha\beta} \frac{\partial f_i}{\partial c_{i\beta}} + \frac{1}{\tau_2} \sum_i -Dn_i + \int \frac{k_B T}{m_i}\frac{1}{f_i}\frac{\partial f_i}{\partial c_{i\alpha}}\frac{\partial f_i}{\partial c_{i\alpha}}, \tag{5.7}$$

where $\tau_{eff} = \tau_2\tau_1/(\tau_2 - \tau_1)$ and $A_{\alpha\beta} = (k_B T/m_i)\delta_{\alpha\beta}$ for the low-Schmidt-number case and $A_{\alpha\beta} = \theta_{\alpha\beta}/m_i$ for the high-Schmidt-number case. Following Singh & Ansumali (2015), (5.7) can be rewritten as

$$\sigma^S = \sum_i \underbrace{\int f_i \frac{\partial \ln(f_i/f_i^*)}{\partial c_{i\alpha}} A_{\alpha\beta} \frac{\partial \ln(f_i/f_i^*)}{\partial c_{i\beta}} \,\mathrm{d}\boldsymbol{c}_i}_{positive} + \sum_i \underbrace{\int \frac{k_B T}{m_i} f_i \left(\frac{\partial \ln(f_i/f_i^*)}{\partial c_{i\alpha}}\right)^2 \mathrm{d}\boldsymbol{c}_i}_{positive}, \tag{5.8}$$

which suggests that

$$\sigma^S \geq 0, \quad \forall\ \tau_1 \leq \tau_2. \tag{5.9}$$

Therefore, the proposed model satisfies the H-theorem for $\tau_1 \leq \tau_2$.

An important condition for Ω^{FP} to be considered valid is that the zero of collision must imply that the distribution function has attained a Maxwell–Boltzmann form. For the present model, the zero of collision, i.e. $\Omega_i^{FP} = 0$, implies

$$\left\langle \Omega_i^{FP(1)}, m_i c_{i\alpha} \right\rangle = 0, \quad \left\langle \Omega_i^{FP(1)}, \frac{m_i c_i^2}{2} \right\rangle = 0, \tag{5.10a,b}$$

then as per (5.5) equilibrium $u_{i\alpha} = u_\alpha$ and $T_i = T$; therefore $\Omega_i^{FP(L)} = 0$ then reduces to

$$\partial_{c_{i\alpha}} \left((c_{i\alpha} - u_\alpha) f_i + \frac{k_B T}{m_i}\frac{\partial f_i}{\partial c_{i\alpha}} \right) = 0. \tag{5.11}$$

Integrating (5.11) with respect to the velocity space and using the fact that the distribution function and its derivatives tend to zero at infinity, we have

$$(c_{i\alpha} - u_\alpha) f_i + \frac{k_B T}{m_i}\frac{\partial f_i}{\partial c_{i\alpha}} = 0. \tag{5.12}$$

https://doi.org/10.1017/jfm.2020.459 Published online by Cambridge University Press

Solving (5.12), we get the Maxwell–Boltzmann distribution as the solution. To find the equilibrium distribution function for the high-Schmidt-number case, we first note that

$$\sum_i \left\langle \Omega_i^{FP(H)}, m_i \xi_{i\alpha} \xi_{i\beta} \right\rangle = \frac{2}{\tau_2} \left(\frac{k_B T}{m_i} - \frac{\theta_{\alpha\beta}}{m_i} \right), \tag{5.13}$$

which suggests that $\Omega^{FP(H)} = 0 \implies \theta_{\alpha\beta}/m_i = (k_B T/m_i)\delta_{\alpha\beta}$. Hence, $\Omega^{FP(H)} = 0$ then reduces to (5.11), the solution for which is the Maxwell–Boltzmann distribution.

Furthermore, the model must be consistent with the indifferentiability principle, i.e. one must be able to recover the Fokker–Planck approximation for the single-component case. In the case where $\tau_1 = \tau_2 = \tau$ and $m_A = m_B = m$, the Fokker–Planck collision kernel for binary mixtures outlined in (5.2) reduces to the approximation for the single-component case, indicating that the proposed model abides by theindifferentiability principle.

As demonstrated above, the proposed model does indeed satisfy the conservation laws, the H-theorem, the zero of collision and the indifferentiability principle. Thus, this model is an acceptable approximation to the Boltzmann equation for binary mixtures.

6. Transport coefficients

In order to obtain the transport coefficients, we perform the Chapman–Enskog expansion, wherein the time derivative, distribution function and other relevant variables are represented as a series, with Kn acting as the smallness parameter (Chapman & Cowling 1970). The distribution function is expressed in series form as

$$f_i = f_i^{MB} + Kn\, f_i^{(1)} + Kn^2 f_i^{(2)} + \cdots, \tag{6.1}$$

with the following constraints imposed on f_i:

$$\left\langle f_i^{(n)}, \left\{ m_i, \sum_{i=A,B} m_i c_{i\alpha}, \sum_{i=A,B} m_i c_i^2/2 \right\} \right\rangle = \{0, \mathbf{0}, 0\}, \quad \forall\, n \geq 1. \tag{6.2}$$

These constraints ensure that component density, mixture momentum and energy are slow moments. The higher-order moments in series form are

$$\left.\begin{aligned} \sigma_{\alpha\beta} &= Kn\, \sigma_{\alpha\beta}^{(1)} + Kn^2\, \sigma_{\alpha\beta}^{(2)} + \cdots, \\ q_\alpha &= Kn\, q_\alpha^{(1)} + Kn^2\, q_\alpha^{(2)} + \cdots, \end{aligned}\right\} \tag{6.3}$$

as the stress and heat flux are zero at equilibrium and are expected to be functions of slow moments otherwise. The time derivative is expressed in series form as

$$\partial_t = \partial_t^{(0)} + Kn\, \partial_t^{(1)} + Kn^2\, \partial_t^{(2)} + \cdots. \tag{6.4}$$

The time derivative of f_i at zeroth order is computed using (Liboff 2003)

$$\partial_t^{(0)} f_i^{MB}(\rho_i, \boldsymbol{u}, T) = \frac{\partial f_i^{MB}}{\partial \rho_i} \partial_t^{(0)} \rho_i + \frac{\partial f_i^{MB}}{\partial \boldsymbol{u}} \partial_t^{(0)} \boldsymbol{u} + \frac{\partial f_i^{MB}}{\partial T} \partial_t^{(0)} T, \tag{6.5}$$

where the expression for the time derivatives of the conserved variables can be calculated from the conservation laws mentioned in (3.10)

https://doi.org/10.1017/jfm.2020.459 Published online by Cambridge University Press

In order to find an expression for the viscosity, we first calculate the stress evolution equation. For the first model it has the form

$$\partial_t \sigma_{\alpha\beta} + \partial_\gamma(\sigma_{\alpha\beta}u_\gamma) + 2p\overline{\partial_\alpha u_\beta} + 2\overline{\sigma_{\alpha\gamma}\partial_\gamma u_\beta} + \partial_\gamma Q_{\alpha\beta\gamma} + \frac{4}{D+2}\overline{\partial_\alpha q_\beta}$$
$$= -\frac{2}{\tau_1}\left(\sigma_{\alpha\beta} + \rho\overline{u_\alpha u_\beta} - \sum_{i=A,B}\rho_i\overline{u_{i\alpha}u_{i\beta}}\right) - \frac{2}{\tau_2}\left(\sum_{i=A,B}\rho_i\overline{u_{i\alpha}u_{i\beta}} - \rho\overline{u_\alpha u_\beta}\right), \tag{6.6}$$

where $Q_{\alpha\beta\gamma} = \sum_{i=A,B}\langle m_i\overline{\xi_{i\alpha}\xi_{i\beta}\xi_{i\gamma}}\rangle$. Retaining terms up to $\mathcal{O}(Kn)$, the stress evolution equation yields

$$2p\overline{\partial_\alpha u_\beta} = -\frac{2\sigma^{(1)}_{\alpha\beta}}{\tau_1}, \tag{6.7}$$

and comparing with the Navier–Stokes law for the stress tensor, we have

$$\mu = \frac{p\tau_1}{2}. \tag{6.8}$$

Similarly, for the second model the right-hand side of the stress evolution equation is

$$\sum_{i=A,B}\langle m_i\overline{\xi_{i\alpha}\xi_{i\beta}}, \Omega_i^{FP(2)}\rangle = -\frac{2}{\tau_2}\sigma_{\alpha\beta}. \tag{6.9}$$

Hence, the expression for viscosity for this model is

$$\mu = \frac{p\tau_2}{2}. \tag{6.10}$$

Similarly, the expression for the diffusion coefficient can be calculated by considering the relaxation of diffusion flux defined as

$$V_\alpha = m_{AB}(u_{A\alpha} - u_{B\alpha}), \tag{6.11}$$

where $m_{AB} = (\rho_A\rho_B)/\rho$. Diffusive flux essentially quantifies the difference between the momentum of a given component and the momentum of the mixture. The series expansion for this quantity is

$$V_\alpha = Kn\, V_\alpha^{(1)} + Kn^2\, V_\alpha^{(2)} + \cdots. \tag{6.12}$$

Similar to stress and heat flux, at equilibrium the diffusive flux attains zero values, as the momenta of both components relax to the mixture momentum. In order to calculate the expression for V_α, we write the expression for individual component velocities. For the first model, we have

$$\left.\begin{aligned}\partial_t\rho_A u_{A\alpha} + \partial_\alpha P_{A\alpha\beta} &= \frac{1}{\tau_2}(\rho u_\alpha - \rho_A u_{A\alpha}),\\ \partial_t\rho_B u_{B\alpha} + \partial_\alpha P_{B\alpha\beta} &= \frac{1}{\tau_2}(\rho u_\alpha - \rho_B u_{B\alpha}),\end{aligned}\right\} \tag{6.13}$$

where $P_{i\alpha\beta} = \langle m_i c_{i\beta}c_{i\beta}\rangle$ and at equilibrium attains the value $P_{i\alpha\beta} = p_i\delta_{\alpha\beta} + \rho_i u_\alpha u_\beta$. After subtracting one equation from the other and collecting terms up to $\mathcal{O}(Kn)$,

https://doi.org/10.1017/jfm.2020.459 Published online by Cambridge University Press

we have

$$\partial_t^{(0)}(\rho_A - \rho_B)u_\alpha + \partial_\beta[(n_A - n_B)k_B T_0 \delta_{\alpha\beta} + (\rho_A - \rho_B)u_\alpha u_\beta] = -\frac{2}{\tau_2} V_{\alpha\beta}^{(1)}. \tag{6.14}$$

The temporal derivatives are replaced using

$$\partial_t^{(0)}\rho_i = -\partial_\alpha(\rho_i u_\alpha), \quad \partial_t^{(0)}\rho u_\alpha = -\partial_\beta(nk_B T_0 \delta_{\alpha\beta} + \rho u_\alpha u_\beta). \tag{6.15a,b}$$

After some rearrangement (6.14) takes the form

$$V_\alpha^{(1)} = \tau_2[Y_A \partial_\alpha p - p\partial_\alpha X_A - X_A \partial_\alpha p], \tag{6.16}$$

where $X_i = n_i/n$ is the component mole fraction and $Y_i = \rho_i/\rho$ is the component mass fraction. Rearranging (6.16) we have

$$\partial_\alpha X_A = -\frac{V_\alpha^{(1)}}{\tau_2 p} + (Y_A - X_A)\frac{\partial_\alpha p}{p}. \tag{6.17}$$

This has the same form as the Stefan–Maxwell equation (Bergman *et al.* 2011), which governs the diffusion in multi-component systems, and for binary mixtures is

$$\partial_\alpha X_A = \frac{X_A X_B}{D_{AB}}\frac{V_\alpha}{m_{AB}} + (Y_A - X_A)\frac{\partial_\alpha p}{p}. \tag{6.18}$$

Comparing (6.17) with the Stefan–Maxwell equation, we get the following expression for the diffusion coefficient:

$$D_{AB} = X_A X_B \frac{p}{m_{AB}}\tau_2. \tag{6.19}$$

The Schmidt number can now be computed as

$$Sc = \frac{\mu}{\rho D_{AB}} = \frac{\tau_1}{2\tau_2}\frac{m_{AB}}{X_A X_B}\frac{1}{\rho} = \frac{\tau_1}{2\tau_2}\frac{Y_A Y_B}{X_A X_B}. \tag{6.20}$$

The existence of the H-theorem for this model suggests that $\tau_1 \leq \tau_2$, hence

$$Sc \leq \frac{Y_A Y_B}{2X_A X_B}. \tag{6.21}$$

This model has an upper limit on the Schmidt number and this is in accordance with the characteristics of the quasi-equilibrium distribution. Similarly, for the second model, the Schmidt number is calculated as

$$Sc = \frac{\mu}{\rho D_{AB}} = \frac{\tau_2}{2\tau_1}\frac{m_{AB}}{X_A X_B}\frac{1}{\rho} = \frac{\tau_2}{2\tau_1}\frac{Y_A Y_B}{X_A X_B}, \tag{6.22}$$

and, since the limitation $\tau_1 \leq \tau_2$ exists, as consistent with the hypothesis, there is a lower bound on the Schmidt number, which is

$$Sc \geq \frac{Y_A Y_B}{2X_A X_B}. \tag{6.23}$$

Hence, both models in conjunction can cover a large range of Schmidt numbers.

https://doi.org/10.1017/jfm.2020.459 Published online by Cambridge University Press

7. Numerical scheme

A Fokker–Planck equation that describes the evolution of the probability density function of the random variable $\boldsymbol{\eta}$ is of the form

$$\frac{\mathrm{d}\mathcal{P}(\boldsymbol{\eta},t)}{\mathrm{d}t} = -\Lambda_\alpha^{(1)}(\boldsymbol{\eta},t)\frac{\partial\mathcal{P}(\boldsymbol{\eta},t)}{\partial\eta_\alpha} + \frac{\zeta_{\alpha\beta}^{(1)}(\boldsymbol{\eta},t)}{2}\frac{\partial^2\mathcal{P}(\boldsymbol{\eta},t)}{\partial\eta_\alpha\partial\eta_\beta} - \Lambda_\alpha^{(2)}(\boldsymbol{\eta},t)\frac{\partial\mathcal{P}(\boldsymbol{\eta},t)}{\partial\eta_\alpha} + \frac{\zeta_{\alpha\beta}^{(2)}}{2}(\boldsymbol{\eta},t)\frac{\partial^2\mathcal{P}(\boldsymbol{\eta},t)}{\partial\eta_\alpha\partial\eta_\beta}, \tag{7.1}$$

where $\boldsymbol{\Lambda}^{(i)}$ are the drift terms and $\boldsymbol{\zeta}^{(i)}$ are the diffusion coefficients. This form of the Fokker–Planck equation is equivalent to the Langevin equation (Risken 1996)

$$\dot{\eta}_\alpha = h_\alpha^{(1)}(\boldsymbol{\eta},t) + g_{\alpha\beta}^{(1)}(\boldsymbol{\eta},t)\Gamma_\beta(t) + h_\alpha^{(2)}(\boldsymbol{\eta},t) + g_{\alpha\beta}^{(2)}(\boldsymbol{\eta},t)\Gamma'_\beta(t), \tag{7.2}$$

where $\boldsymbol{h}^{(i)}$ are the drift terms, $\boldsymbol{g}^{(i)}$ are the diffusion coefficients, and $\boldsymbol{\Gamma}$, $\boldsymbol{\Gamma}'$ are Gaussian distributed random numbers that have the following properties:

$$\langle\Gamma_\alpha(t)\rangle = 0, \quad \langle\Gamma_\alpha(t)\Gamma_\beta(t')\rangle = \delta(t-t')\delta_{\alpha\beta}. \tag{7.3a,b}$$

Under these conditions, the following relations hold (Risken 1996):

$$\left.\begin{aligned}\Lambda_\alpha^{(1)} &= h_\alpha^{(1)}(\boldsymbol{\eta},t), \quad \zeta_{\alpha\beta}^{(1)} = g_{\alpha\gamma}^{(1)}g_{\gamma\beta}^{(1)},\\ \Lambda_\alpha^{(2)} &= h_\alpha^{(2)}(\boldsymbol{\eta},t), \quad \zeta_{\alpha\beta}^{(2)} = g_{\alpha\gamma}^{(2)}g_{\gamma\beta}^{(2)}.\end{aligned}\right\} \tag{7.4}$$

The central idea is that the solution to the Fokker–Planck equation is approximated by considering an ensemble of trajectories generated by the Langevin dynamics. In this case, a large number of particles have their positions and velocities updated using (7.2). We now discuss the numerical scheme for the two cases.

7.1. *Low-Schmidt-number limit*

For the first model, the equivalent Langevin equations are

$$\left.\begin{aligned}\frac{\mathrm{d}x_\alpha}{\mathrm{d}t} &= c_{i\alpha},\\ \frac{\mathrm{d}c_{i\alpha}}{\mathrm{d}t} &= -\left(\frac{1}{\tau_{eff}}\right)(c_{i\alpha}-u_{i\alpha}) - \frac{1}{\tau_2}(c_{i\alpha}-u_\alpha) + \sqrt{\frac{2k_BT_i}{m_i}}\,\mathrm{d}W_\alpha + \sqrt{\frac{2k_BT}{m_i}}\,\mathrm{d}W'_\alpha,\end{aligned}\right\} \tag{7.5}$$

where $\mathrm{d}W_\alpha$ and $\mathrm{d}W'_\alpha$ denote random forces with the following statistics:

$$\langle\mathrm{d}W_\alpha\rangle = 0, \quad \langle\mathrm{d}W'_\alpha\rangle = 0, \quad \langle\mathrm{d}W_\alpha\,\mathrm{d}W'_\alpha\rangle = 0. \tag{7.6a,b}$$

More specifically, $\mathrm{d}W = W(t+\Delta t) - W(t)$ is the standard Weiner process, where $W(t)$ is a rapidly changing random force with mean and variance as (Gardiner 1985)

$$\langle\mathrm{d}W_\alpha(t)\rangle = 0, \quad \langle\mathrm{d}W_\alpha\,\mathrm{d}W_\beta\rangle = \mathrm{d}t\,\delta_{\alpha\beta}. \tag{7.7a,b}$$

Thus, the detailed binary collision description is approximated by a random collision with a heat bath in the model.

https://doi.org/10.1017/jfm.2020.459 Published online by Cambridge University Press

These Langevin equations can be solved efficiently using the stochastic version of the Verlet algorithm. For the present model, the discretization scheme we have used is (Kloeden & Platen 2013; Singh & Ansumali 2015)

$$\left.\begin{aligned} x_\alpha^{(1)} &= x_\alpha(t) + \frac{1}{2}c_{i\alpha}(t)\Delta t, \\ c_{i\alpha}(t+\Delta t) = c_{i\alpha}(t) &- \left(\frac{\vartheta_1}{1+\vartheta_1/2}\right)(c_{i\alpha}(t)-u_{i\alpha}) - \left(\frac{\vartheta_2}{1+\vartheta_2/2}\right)(c_{i\alpha}(t)-u_\alpha) \\ &+ \frac{\sqrt{2\mathcal{D}_i^{(1)}\vartheta_1}}{1+\vartheta_1/2}\phi_\alpha + \frac{\sqrt{2\mathcal{D}_i^{(2)}\vartheta_2}}{1+\vartheta_2/2}\phi'_\alpha, \\ x_\alpha(t+\Delta t) &= x_\alpha^{(1)} + \frac{1}{2}c_{i\alpha}(t+\Delta t)\Delta t, \end{aligned}\right\} \tag{7.8}$$

where $\vartheta_1 = \Delta t/\tau_{eff}$, $\vartheta_2 = \Delta t/\tau_2$, ϕ_α and ϕ'_α are Gaussian random numbers with mean zero and variance unity, and $\mathcal{D}_i^{(1)}$ and $\mathcal{D}_i^{(2)}$ are k_BT_i/m_i and k_BT/m_i, respectively. The recently proposed Molecular Dice algorithm (Agrawal, Bhattacharya & Ansumali 2018) was used to generate these Gaussian random numbers, which indicated considerable increase in efficiency without any loss of accuracy. This scheme works efficiently for small time steps such that $\max\{\vartheta_1, \vartheta_2\} \leq 0.001$.

7.2. *High-Schmidt-number limit*

The formulation for this model remains largely unchanged and the equivalent Langevin equations are

$$\left.\begin{aligned} \frac{\mathrm{d}x_\alpha}{\mathrm{d}t} &= c_{i\alpha}, \\ \frac{\mathrm{d}c_{i\alpha}}{\mathrm{d}t} &= -\left(\frac{1}{\tau_{eff}}\right)(c_{i\alpha}-u_\alpha) - \frac{1}{\tau_2}(c_{i\alpha}-u_\alpha) + \sqrt{2}\theta'_{i\alpha\beta}\,\mathrm{d}W_\beta + \sqrt{\frac{2k_BT}{m_i}}\,\mathrm{d}W'_\alpha, \end{aligned}\right\} \tag{7.9}$$

where $\theta'_{i\alpha\gamma}\theta'_{i\gamma\beta} = \theta_{i\alpha\beta}/m_i$ and $\theta'_{\alpha\beta}$ can be calculated by using Cholesky decomposition of $\theta_{\alpha\beta}/m_i$. The discretization scheme for this model is

$$\left.\begin{aligned} x_\alpha^{(1)} &= x_\alpha(t) + \frac{1}{2}c_{i\alpha}(t)\Delta t, \\ c_{i\alpha}(t+\Delta t) = c_{i\alpha}(t) &- \left(\frac{\vartheta_1}{1+\vartheta_1/2}\right)(c_{i\alpha}(t)-u_\alpha) - \left(\frac{\vartheta_2}{1+\vartheta_2/2}\right)(c_{i\alpha}(t)-u_\alpha) \\ &+ \frac{\sqrt{2\vartheta_1}\theta'_{i\alpha\beta}}{1+\vartheta_1/2}\phi_\beta + \frac{\sqrt{2\mathcal{D}_i^{(2)}\vartheta_2}}{1+\vartheta_2/2}\phi'_\alpha, \\ x_\alpha(t+\Delta t) &= x_\alpha^{(1)} + \frac{1}{2}c_{i\alpha}(t+\Delta t)\Delta t. \end{aligned}\right\} \tag{7.10}$$

In order to validate the numerical scheme, we started with a mixture with $m_B/m_A = 2$ with $N = 10^5$ particles in a single periodic box. For model I, the velocities of the lighter particles were initialized uniformly in the range [0, 1) and the heavier particles in the range [0, 2). For model II, the velocities of the lighter particles were initialized with a Gaussian

https://doi.org/10.1017/jfm.2020.459 Published online by Cambridge University Press

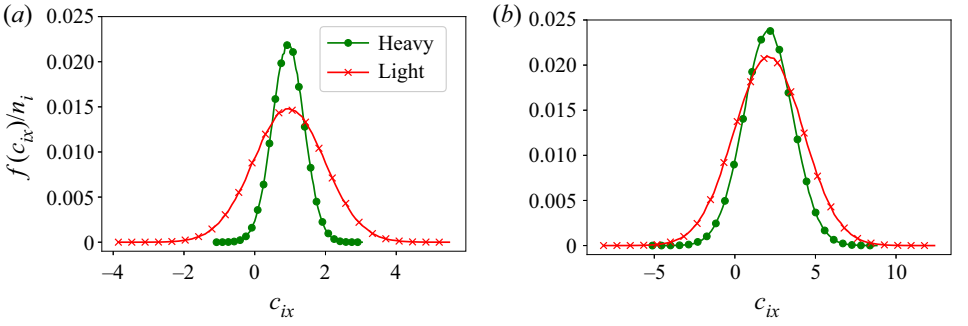


FIGURE 3. Plot of the distribution of velocities of the light and heavy components at equilibrium for (*a*) model I and (*b*) model II.

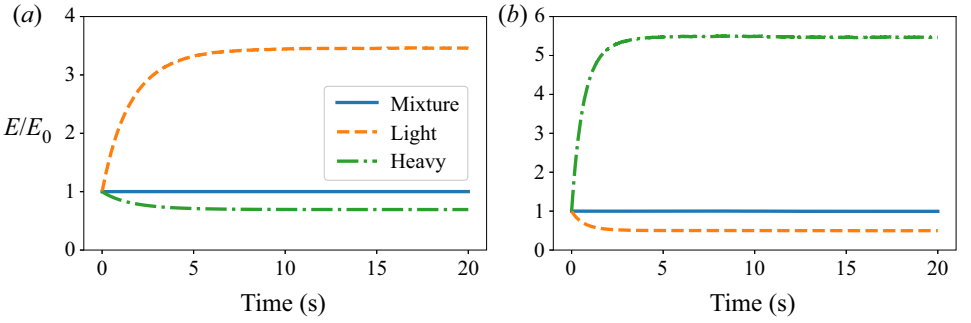


FIGURE 4. Plot of the ratio of energy at time t to the initial energy ($E(t)/E_0$) versus time for individual components and the mixture for (*a*) model I and (*b*) model II.

distribution with mean 4 and variance 10, and the heavier particles were Gaussian distributed with mean 1 and variance 1. The plots of energy of the two components and the mixture with time averaged over an ensemble of 15 trajectories and the distribution of velocities in a particular direction, for both cases, are shown in figures 3 and 4.

8. Simulation results

In this section, we present the results for three benchmark problems: Graham's law for effusion, Couette flow and binary diffusion.

8.1. *Graham's law for effusion*

Effusion is a process wherein gas molecules escape through a small hole. The length parameter of this hole is much smaller than the mean free path of the gas, i.e. $d \ll \lambda_{mfp}$. A sketch of the process is shown in figure 5. The number flux of the gas through this small hole is

$$\Phi_i = \langle c_{iz}, f(\boldsymbol{c}_i)\rangle, \tag{8.1}$$

where Φ_i is the number flux and c_{iz} is the molecular velocity in the direction perpendicular to the plane of the hole. By integrating over velocity space, facilitated by a shift to the

https://doi.org/10.1017/jfm.2020.459 Published online by Cambridge University Press

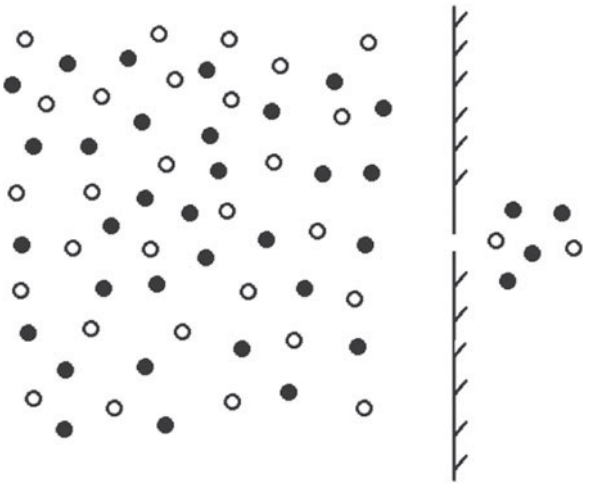


FIGURE 5. The lighter particles (in this case filled circles) escape through the hole faster than the heavier particles, with a factor proportional to the square root of their mass ratios.

spherical coordinate system, the expression for Φ_i is

$$\Phi_i = \frac{P}{\sqrt{2\pi m_i k_B T}}, \tag{8.2}$$

where P is the pressure and T is the temperature of the gas. Then, for a well-mixed binary mixture, the ratio of the fluxes is (Mason & Kronstadt 1967)

$$\frac{\Phi_A}{\Phi_B} = \sqrt{\frac{m_B}{m_A}}. \tag{8.3}$$

We simulated this system for three mass ratios, i.e. $m_B/m_A = 4$, $m_B/m_A = 16$ and $m_B/m_A = 100$. The boundary conditions in the transverse directions were taken to be periodic while maintaining constant pressure in the system. The results have been plotted in figure 6. As can be seen, the simulations are in excellent agreement with the analytical solution.

8.2. *Couette flow*

The set-up of the problem is simple: fluid between two plates is sheared in opposite directions with equal magnitudes. A sketch of the problem is shown in figure 7. In order to validate the model, we calculate the global stress tensor defined as (Sharipov, Cumin & Kalempa 2004)

$$\Pi = -\frac{v_0}{2UP_0} P_{xy}, \tag{8.4}$$

where $P_0 = nk_BT_0$ is the reference pressure. This quantity is calculated in the entire range of rarefaction parameter, δ, which is the inverse of the Knudsen number and is defined as

$$\delta = \frac{HP_0}{\mu v_0}, \tag{8.5}$$

https://doi.org/10.1017/jfm.2020.459 Published online by Cambridge University Press

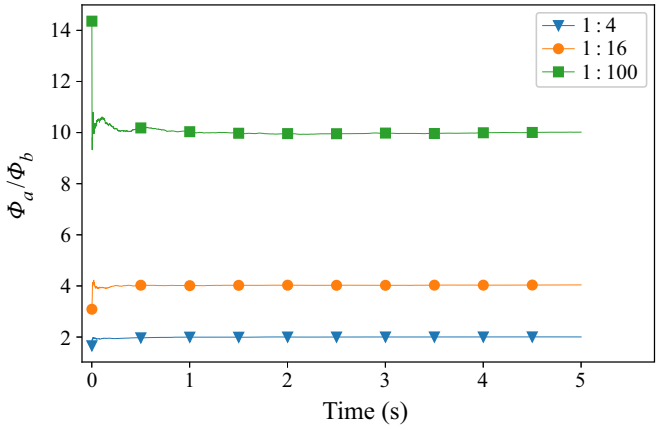


FIGURE 6. Model I was used to simulate a set-up that could mimic Graham's law for effusion. The results observed are in very good agreement with the expected behaviour, for all three cases.

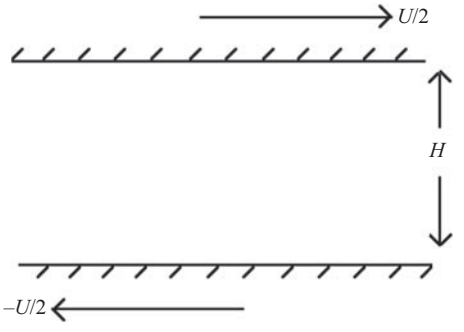


FIGURE 7. A representative sketch of the Couette flow set-up. Two walls with a separation H are sheared in opposite directions with velocity $U/2$.

where μ is the mixture viscosity and v_0 is the characteristic molecular velocity of the mixture, defined as

$$v_0 = \sqrt{\frac{2k_B T_0}{m_0}}, \tag{8.6}$$

where $m_0 = C_0 m_A + (1 - C_0)m_B$, with C_0 being the concentration of the lighter component. We simulated the system for three mixtures, neon–argon (Ne–Ar), helium–argon (He–Ar) and helium–xenon (He–Xe), for rarefaction parametersin the range [0.01, 40] for three different concentrations (0.1, 0.5, 0.9). The value for Π was computed by averaging over 10^5 iterations for each parameter and the results are tabulated in table 1. The error bar (standard deviation) was of the same order for all parameters and in the range [0.00478, 0.00544]. The results were found to be in good agreement with the reported results of Sharipov *et al.* (2004). This indicates that the proposed method is indeed capable of simulating flows in a wide range of Knudsen numbers.

https://doi.org/10.1017/jfm.2020.459 Published online by Cambridge University Press

	Ne–Ar			He–Ar			He–Xe		
δ	$C_0 = 0.1$	0.5	0.9	0.1	0.5	0.9	0.1	0.5	0.9
0.01	0.27558	0.27266	0.27471	0.27004	0.24510	0.24381	0.26694	0.22559	0.19842
0.1	0.25295	0.25014	0.25216	0.24764	0.22383	0.22296	0.24442	0.20483	0.17994
1.0	0.16539	0.16324	0.16458	0.16141	0.14455	0.14650	0.15835	0.12959	0.11892
10.0	0.04141	0.04124	0.04159	0.04054	0.03886	0.04055	0.04091	0.03526	0.03706
40.0	0.01222	0.01219	0.01196	0.01220	0.01185	0.01217	0.01125	0.01165	0.01155

TABLE 1. The Π values for Ne–Ar, He–Ar and He–Xe mixtures for three different compositions.

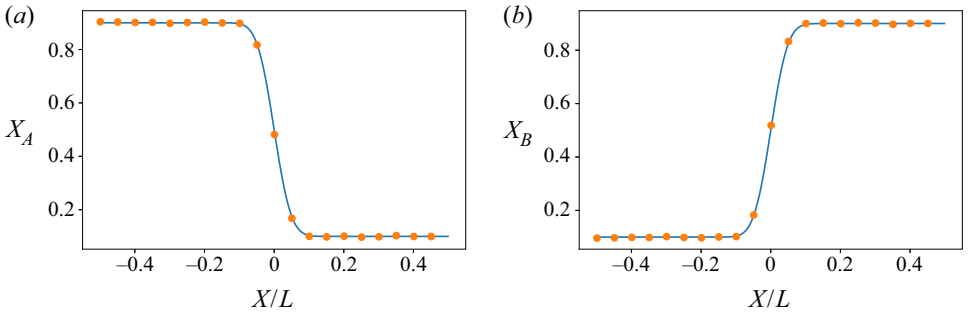


FIGURE 8. Plot of the concentrations after 20 000 time steps of the component (*a*) A and (*b*) B, compared with the analytical solution given by (8.8).

8.3. *Binary diffusion*

The profile of the mixture in this set-up is determined by the step function

$$\left.\begin{array}{ll} X_A = 90\,\%, & X_B = 10\,\% \quad \text{if } x < 0, \\ X_B = 10\,\%, & X_B = 90\,\% \quad \text{if } x \geq 0, \end{array}\right\} \tag{8.7}$$

where the mass ratio of the components was chosen to be $m_B/m_A = 5$. The step function is used instead of a smooth profile as it is a more severe check for the numerical scheme. Under the assumption that, at infinity, the initial concentrations remains unchanged, this problems yields the analytical solution (Bergman *et al.* 2011)

$$X_i = \left[\frac{1}{2} + \frac{\Delta X_i}{2}\,\mathrm{erf}\left(\frac{x}{\sqrt{4D_{AB}t}}\right)\right], \tag{8.8}$$

where D_{AB} is the diffusion constant. The simulation was done for 20 000 time steps, and the plots for both components compared against their respective analytical solutions are plotted in figure 8. The simulation results were very close to the analytical solution. This exercise proves that the value of D_{AB} set by the numerical scheme is accurate.

9. Outlook

We have developed a new thermodynamically consistent Fokker–Planck approximation to the Boltzmann equation for binary gas mixtures, based on quasi-equilibrium models.

https://doi.org/10.1017/jfm.2020.459 Published online by Cambridge University Press

These models were subjected to numerical experiments, like Graham's law, Couette flow and binary diffusion, and it was determined that the algorithm is capable of simulating flow for a wide range of Knudsen numbers and diffusion coefficients.

Finally, we wish to point out that this Fokker–Planck model of binary mixtures needs to be extended for multi-component mixtures and possibly to reactive systems due to its practical relevance related to reaction–diffusion systems. This extension, though it is conceptually straightforward, does require some new technical ingredients. We leave the development of such a model to future work, but we would like to highlight some of these technicalities before concluding. A straightforward model for an $\mathcal{N}$-component mixture model can be formulated by introducing separate relaxation times and quasi-equilibrium for each component in the proposed collision approximation (5.2). One would expect that most characteristics of the current model will be preserved by such an extension. The tunable relaxation time is obtained by comparing the hydrodynamic limit of the kinetic equation with its macroscopic counterpart, the Stefan–Maxwell diffusion equation for an isothermal system. However, as the diffusion coefficient is an $\mathcal{N} \times \mathcal{N}$ symmetric matrix while the number of tunable parameters is only $\mathcal{N}$, such a representation is not complete. This issue can be resolved by utilizing the mixture-averaged diffusion approximation (Bird, Stewart & Lightfoot 1960). Such formulations are correct only asymptotically when there is either only one bulk component and $\mathcal{N} - 1$ trace species, or when all species but one have nearly the same diffusion coefficient. A more detailed model should introduce $\mathcal{N}(\mathcal{N} - 1)/2$ independent relaxation times. We leave it to future work to explore these issues and possibly extend the model to also incorporate chemical reactions in the kinetic equation framework.

Acknowledgments

S.K.S. expresses his sincere thanks to the Department of Science and Technology (DST), SERB, India, for financial support under the Young Scientist Scheme (S. No. YSS/2015/002085). S.An. expresses his sincere thanks to the Department of Science and Technology, India, for financial assistance (S. No. SB2/S2/CMP-056/2013). The authors would like to acknowledge M. Atif for his help with the figures.

Declaration of interests

The authors report no conflict of interest.

REFERENCES

AGRAWAL, S., BHATTACHARYA, S. & ANSUMALI, S. 2018 Molecular dice: random number generators á la Boltzmann. *Phys. Rev.* E **98** (6), 063315.

ARCIDIACONO, S., KARLIN, I., MANTZARAS, J. & FROUZAKIS, C. 2007 Lattice Boltzmann model for the simulation of multicomponent mixtures. *Phys. Rev.* E **76** (4), 046703.

ARCIDIACONO, S., MANTZARAS, J., ANSUMALI, S., KARLIN, I., FROUZAKIS, C. & BOULOUCHOS, K. 2006 Simulation of binary mixtures with the lattice Boltzmann method. *Phys. Rev.* E **74** (5), 056707.

BERGMAN, T. L., INCROPERA, F. P., DEWITT, D. P. & LAVINE, A. S. 2011 *Fundamentals of Heat and Mass Transfer*. Wiley.

BHATNAGAR, P. L., GROSS, E. P. & KROOK, M. 1954 A model for collision processes in gases. I. Small amplitude processes in charged and neutral one-component systems. *Phys. Rev.* **94** (3), 511.

BIRD, R., STEWART, W. & LIGHTFOOT, E. 1960 *Transport Phenomena*. Wiley.

https://doi.org/10.1017/jfm.2020.459 Published online by Cambridge University Press

CHAPMAN, S. & COWLING, T. G. 1970 *The Mathematical Theory of Non-uniform Gases: An Account of the Kinetic Theory of Viscosity, Thermal Conduction and Diffusion in Gases*. Cambridge University Press.

GARDINER, C. W. 1985 *Handbook of Stochastic Methods*. Springer.

GORBAN, A. N. & KARLIN, I. V. 1994*a* General approach to constructing models of the Boltzmann equation. *Physica* **206** (3–4), 401–420.

GORBAN, A. N. & KARLIN, I. V. 1994*b* Method of invariant manifolds and regularization of acoustic spectra. *Transp. Theory Stat. Phys.* **23** (5), 559–632.

GORJI, H. & JENNY, P. 2012 A kinetic model for gas mixtures based on a Fokker–Planck equation. *J. Phys.: Conf. Ser.* **362**, 012042.

GORJI, M. H. & JENNY, P. 2014 An efficient particle Fokker–Planck algorithm for rarefied gas flows. *J. Comput. Phys.* **262**, 325–343.

GORJI, M. H., TORRILHON, M. & JENNY, P. 2011 Fokker–Planck model for computational studies of monatomic rarefied gas flows. *J. Fluid Mech.* **680**, 574–601.

GRAD, H. 1949 On the kinetic theory of rarefied gases. *Commun. Pure Appl. Maths* **2** (4), 331–407.

HAMEL, B. B. 1965 Kinetic model for binary gas mixtures. *Phys. Fluids* **8** (3), 418–425.

HOLWAY, L. H. JR. 1966 New statistical models for kinetic theory: methods of construction. *Phys. Fluids* **9** (9), 1658–1673.

KLOEDEN, P. E. & PLATEN, E. 2013 *Numerical Solution of Stochastic Differential Equations*, vol. 23. Springer Science & Business Media.

LEBOWITZ, J. L., FRISCH, H. L. & HELFAND, E. 1960 Nonequilibrium distribution functions in a fluid. *Phys. Fluids* **3** (3), 325–338.

LEVERMORE, C. D. 1996 Moment closure hierarchies for kinetic theories. *J. Stat. Phys.* **83** (5–6), 1021–1065.

LIBOFF, R. L. 2003 *Kinetic Theory: Classical, Quantum, and Relativistic Descriptions*. Springer Science & Business Media.

LIFSCHITZ, E. & PITAEVSKII, L. 1981 *Physical Kinetics*. Pergamon.

MASON, E. & KRONSTADT, B. 1967 Graham's laws of diffusion and effusion. *J. Chem. Educ.* **44** (12), 740.

RISKEN, H. 1996 *The Fokker–Planck Equation*, pp. 63–95. Springer.

SHARIPOV, F., CUMIN, L. M. G. & KALEMPA, D. 2004 Plane couette flow of binary gaseous mixture in the whole range of the Knudsen number. *Eur. J. Mech.* B/*Fluids* **23** (6), 899–906.

SINGH, S. K. & ANSUMALI, S. 2015 Fokker–Planck model of hydrodynamics. *Phys. Rev.* E **91** (3), 033303.

SINGH, S. K., THANTANAPALLY, C. & ANSUMALI, S. 2016 Gaseous microflow modeling using the Fokker–Planck equation. *Phys. Rev.* E **94** (6), 063307.

https://doi.org/10.1017/jfm.2020.459 Published online by Cambridge University Press